



HAL
open science

Long-term thermo-mechanical behaviour of energy piles in clay

van Tri Nguyen, Nanwangzi Wu, Yixiang Gan, Jean-Michel Pereira, Anh
Minh A.M. Tang

► **To cite this version:**

van Tri Nguyen, Nanwangzi Wu, Yixiang Gan, Jean-Michel Pereira, Anh Minh A.M. Tang. Long-term thermo-mechanical behaviour of energy piles in clay. *Environmental Geotechnics*, 2020, 7 (4), pp.237-248. 10.1680/jenge.17.00106 . hal-02879341

HAL Id: hal-02879341

<https://enpc.hal.science/hal-02879341>

Submitted on 23 Jun 2020

HAL is a multi-disciplinary open access archive for the deposit and dissemination of scientific research documents, whether they are published or not. The documents may come from teaching and research institutions in France or abroad, or from public or private research centers.

L'archive ouverte pluridisciplinaire **HAL**, est destinée au dépôt et à la diffusion de documents scientifiques de niveau recherche, publiés ou non, émanant des établissements d'enseignement et de recherche français ou étrangers, des laboratoires publics ou privés.

1 **Long-term thermo-mechanical behaviour of energy pile in clay**

2 V. T. NGUYEN ¹, N. WU ², Y. GAN ², J. M. PEREIRA ¹, A. M. TANG ¹

3 ¹ *Laboratoire Navier, UMR 8205, École des Ponts ParisTech, IFSTTAR, CNRS, UPE, France*

4 ² *School of Civil Engineering, The University of Sydney, NSW 2006, Australia*

5

6 **Corresponding author:**

7 Dr. Anh Minh TANG

8

9 Ecole des Ponts ParisTech

10 Laboratoire Navier/Géotechnique (CERMES)

11 6-8 avenue Blaise Pascal

12 77455 MARNE-LA-VALLEE

13 France

14 Tel: +33.1.64.15.35.63

15 <http://navier.enpc.fr>

16 Email: anhminh.tang@enpc.fr

17

18

19 ABSTRACT

20 In engineering practice, energy pile foundations are often designed for the lifetime of the
21 building. Thermal exchange between a pile and the surrounding soil depends on the annual
22 energy needs of the building, as heating mode in winter and cooling mode in summer. Thus,
23 energy pile foundations will undergo a heating-cooling cycle per year. In the present work, an
24 experimental method based on a small-scale pile model installed in saturated clay was used to
25 study the thermo-mechanical behaviour of energy pile under thermal cycles. 30 cycles were
26 applied (to represent a 30-year period if we neglect the daily cycles) while the pile head load
27 was maintained constant. Four tests were performed corresponding to pile head loads equal to
28 0, 20%, 40% and 60% of pile resistance. The results obtained show the increase of
29 irreversible pile head settlement with the thermal cycles. In order to better interpret the
30 experimental results, the finite element method is used to simulate numerically the
31 experiments. That allows highlighting the important role of pile thermal
32 contraction/expansion in the pile/soil interaction under thermo-mechanical loading.

33 KEYWORDS: energy pile, numerical modelling, physical modelling, saturated clay, thermal
34 cycles, thermo-mechanical behaviour.

35

36 INTRODUCTION

37

38 Pile foundations are used to erect a structure on an underground with poor load bearing
39 properties. The energy piles (also called “heat exchanger piles”) are the foundation piles that
40 are used also as heat exchangers. A system of heat exchanger pipes is embedded in such piles
41 allowing the exchanges of thermal energy between the ground and the building via a fluid
42 circulating in the pipes. This system combined with a heat pump allows extracting heat from
43 the soil in winter and re-injecting back heat to the soil in summer (Abuel-Naga *et al.*, 2015;

44 de Santayanal *et al.*, 2019). Thus, energy pile foundation is subjected to a heating-cooling
45 cycle per year, which reflects seasonal temperature variations. These annual thermal cycles
46 would then modify the soil/pile interaction from the thermo-mechanical point of view. In
47 spite of various studies on the thermo-mechanical behaviour of energy piles, few works have
48 investigated their long-term behaviour. Actually, to deal with this aspect, some studies
49 investigated the mechanical behaviour of energy piles subjected to numerous thermal cycles,
50 which represent the seasonal pile temperature variations (Ng *et al.*, 2014; Pasten and
51 Santamarina, 2014; Suryatriyastuti *et al.*, 2014; Di Donna and Laloui, 2015; Olgun *et al.*,
52 2015; Saggiu and Chakraborty, 2015; Ng *et al.*, 2016; Bidarmaghz *et al.*, 2016; Vieira and
53 Maranha, 2016; Nguyen *et al.*, 2017). In these studies, numerical methods are usually used
54 and experimental methods are mainly based on physical modelling.

55

56 Among the numerical methods, the conventional load transfer method is the simplest one.
57 Suryatriyastuti *et al.* (2014) used this method, combined with additional mechanisms for
58 predicting degradation behaviour of pile-soil interface under thermal cycles, and investigated
59 the behaviour of free- and restraint-head pile in loose sand. The results show a ratcheting of
60 pile head settlement under a constant working load and a decrease in pile head force for the
61 restraint-head pile after 12 thermal cycles. Pasten and Santamarina (2014) developed a
62 modified one-dimensional load transfer model to predict the displacement of pile elements.
63 The results show that the axial force changes mainly in the middle of pile length when the
64 pile works under a heating phase. But in a cooling phase the axial force changes are
65 negligible. Besides, the irreversible settlement of pile reaches a plateau after several thermal
66 cycles.

67 Besides the load transfer method, the finite element method is also used to investigate long-
68 term thermo-mechanical behaviour of energy piles. Saggiu and Chakraborty (2015)

69 investigated the behaviour of a floating and end-bearing pile in loose and dense sand under
70 various thermal cycles by using the finite element method. The result shows an important
71 settlement of the pile after the first thermal cycle. A similar result can be found in the
72 numerical study of Olgun *et al.* (2015) where pile head displacement and axial stress were
73 investigated under three different climatic conditions for 30 years. After 30 annual thermal
74 cycles, even if the pile was progressively cooled, the axial stress along the pile tended to
75 increase. A decrease in axial stress was observed during heating. This was explained by the
76 difference in the thermal dilation between the pile and the soil during the thermal loading
77 process. Ng *et al.* (2016) studied the horizontal stress change of soil element close to the pile
78 when the pile is subjected to 50 heating-cooling cycles. The results show that the horizontal
79 stress along the pile depth decreased with thermal cycles. In addition, the irreversible
80 settlement of pile due to the decrease of the shaft resistance leads to the densification of soil
81 below the pile toe and thus the decrease of the rate of pile's settlement.

82 Few studies have investigated the long-term thermo-mechanical behaviour of energy pile in
83 clay. Di Donna and Laloui (2015) have developed a numerical model to estimate the
84 additional displacement of pile and stress-strain state at the soil-pile interface. The result
85 indicates that the upper part of pile heaves in the heating phase and settles in the cooling
86 phase. The irreversible settlement of the pile is observed in the first cycle, but in the
87 following cycles the vertical displacement of the pile is almost reversible. A greater plastic
88 strain was obtained within the soil mass at points located close to the soil-pile interface.

89 Vieira and Maranhã (2016) investigated the behaviour of a floating pile model in clay soil
90 under different constant static loads and seasonal temperature variations during five years
91 using the finite element method. The considered soil is saturated and normally consolidated.
92 The results indicate that when the pile works with a high factor of safety, its displacement is

93 reversible during the thermal cycles. However, a low factor of safety induces an increase in
94 axial stresses while the rate of irreversible settlement reduces with the number of cycles.

95

96 Beside the numerical studies mentioned above, few experimental studies have been
97 performed to investigate the long-term behaviour of energy piles in clay. Ng *et al.* (2014)
98 used centrifuge modelling to study the thermo-mechanical behaviour of energy piles
99 constructed in lightly and heavily over-consolidated clay under five thermal cycles. The
100 results show that the most irreversible settlement of pile was observed in the first thermal
101 cycle, and then in the following cycles the settlement increases at a lower rate. After 5 cycles
102 the cumulative settlement was about $3.8\% \cdot D$ (D being the pile diameter) for a pile in the
103 lightly over-consolidated clay, and $2.1\% \cdot D$ in the case of heavily over-consolidated clay.

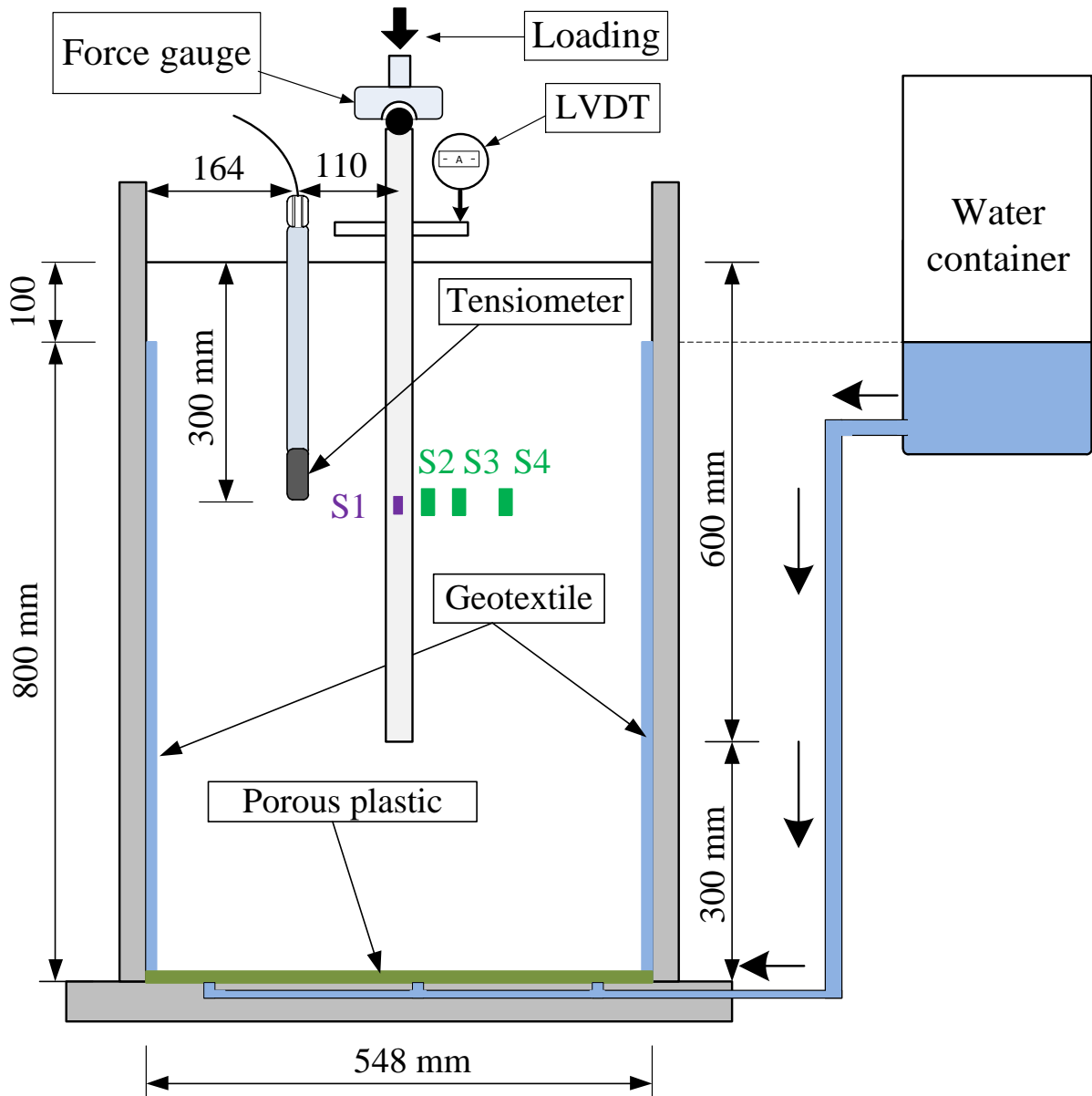
104

105 In the present work, the long-term thermo-mechanical behaviour of an energy pile in clay is
106 investigated both by physical and numerical modelling. First, a small-scale pile model
107 installed in saturated clay was used. 30 thermal cycles were applied while the pile head load
108 was maintained constant at 0, 20%, 40% and 60% of pile bearing capacity. Second, the finite
109 element method is used to simulate numerically the experiments. The results of the two
110 methods are finally analysed simultaneously to better identify the main mechanisms
111 controlling the thermo-mechanical behaviour of energy pile under several thermal cycles. The
112 novelty of the work consists in integrating results of a small-scale pile model (physical
113 modelling) with those obtained by numerical modelling (finite element numerical model). As
114 referred above few (and very recent) works can be found in the literature dealing with the
115 long-term mechanical effect on energy geostructures (energy piles, in the present case) under
116 thermal cycles.

117

118 PHYSICAL MODELING

119 The pile model is made of an aluminium tube with internal and external diameters of 18 mm
120 and 20 mm, respectively. The length of the tube is 800 mm and it is sealed at the bottom. Its
121 external surface was coated with sand to imitate the roughness of a full-scale bored pile. 600
122 mm of the pile was embedded in saturated clay (see Figure 1).



S1: Temperature transducer inside the pile
S2÷4: Temperature transducer distributed in soil

123

124

Figure 1. Experiment setup

125

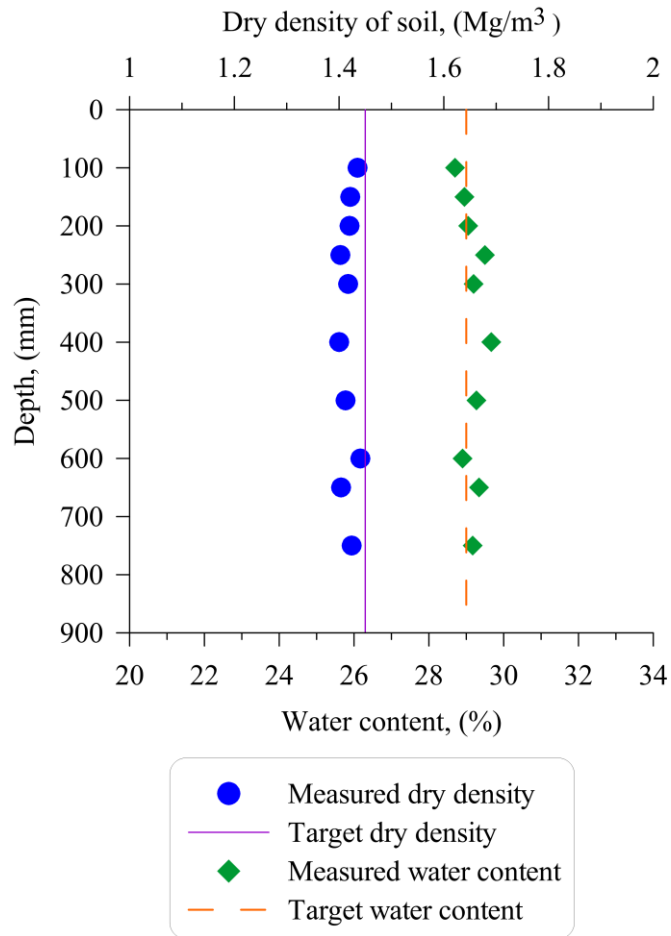
126 The pile temperature is controlled by a metallic U-tube inserted inside it and connected to a
127 cryostat. A temperature sensor (accuracy equals $\pm 0.01^\circ\text{C}$) is embedded inside the pile, at 300-
128 mm depth, to monitor its temperature during the experiments. The axial load applied to the
129 pile head is controlled by deadweight (more details can be found in Yavari *et al.*, 2014 on a
130 similar setup) and measured by a force sensor. The pile head displacement is measured by a
131 displacement sensor (LVDT) with an accuracy of ± 0.001 mm. Temperature in soil is
132 measured by three sensors embedded at 300-mm depth and 20, 40, 80 mm from the pile axis.

133

134 Speswhite Kaolin clay was used in this study. It has a clay fraction of 30%, a liquid limit of
135 57%, a plastic limit of 33% and a particle density of 2.60 Mg/m^3 . Clay powder was mixed
136 with water by using a soil mixer to achieve a water content of 29%. It is then stored in a
137 sealed box for one month for moisture homogenization. Compaction was performed, by layer
138 of 50-mm thickness, using an electrical vibratory hammer. The soil mass used for the
139 compaction of each layer was controlled to obtain a dry density of 1.45 Mg/m^3 (degree of
140 saturation equals 95% and void ratio equals 0.79). After the compaction of the first six layers,
141 the model pile was installed in place, and the remaining soil layers were completed. At the
142 vicinity of the pile model, a small metal hammer was used to avoid damaging the pile.

143

144 To control the quality of the compaction procedure, soil samples (20 mm in diameter) were
145 cored from the compacted soil mass for the determination of dry density and water content.
146 The created hole was refilled afterwards prior to the test with energy pile. Results show that
147 the dry density and the water content are relatively uniform with depth and they are close to
148 the target values (Figure 2).



149

150

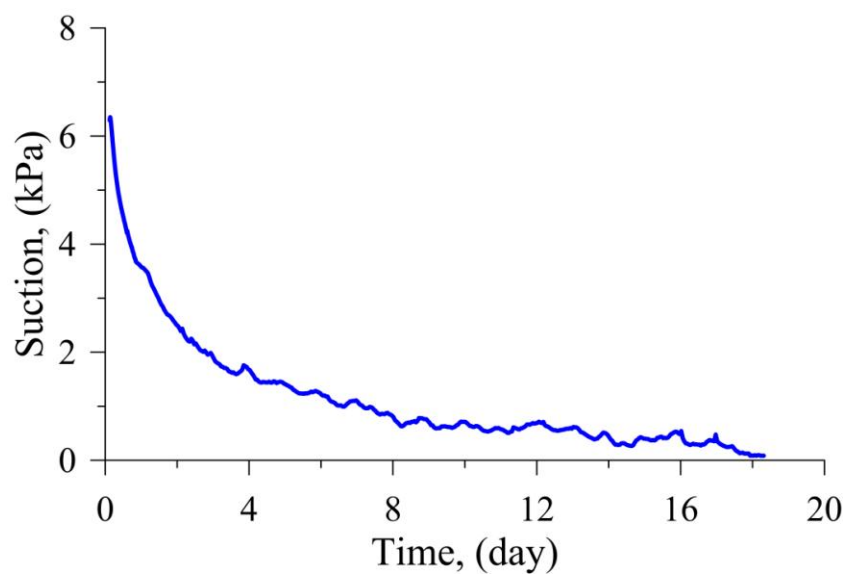
Figure 2. Dry density and water content of compacted soil

151

152 In the work of Yavari *et al.* (2016a), re-saturating a similar soil mass from the bottom took
 153 several months. In the present work, to speed up this phase, a porous plastic plate was
 154 installed at the bottom of the soil container and a thin geotextile layer was installed between
 155 the container internal surface and the soil mass (see Figure 1). Thus, water from the container
 156 can easily flow through the small holes at the bottom of the soil container and diffuse into the
 157 soil mass via the porous plastic plate and the surrounding geotextile. The water level in the
 158 water container was kept 100-mm below the soil surface to avoid water overflow on the soil
 159 surface. During the saturation, a tensiometer T8 (T8-UMS, 2008) was used to control the soil
 160 suction at 300-mm depth and 110-mm far from the pile's axis (see Figure 1). Result in the
 161 Figure 3 shows that after 18 days of saturation the soil suction at the tensiometer position is

162 very close to zero. The tensiometer was then removed and the resulting hole was refilled to
163 avoid its influence on the thermo-mechanical behaviour of the pile. The saturation process
164 was kept for 45 days in total to ensure the full saturation of the soil mass. It should be noted
165 that, during the saturation, the soil container was covered on its surface to avoid water
166 evaporation and heat exchange. Moreover, the saturation system was maintained during the
167 subsequent thermo-mechanical experiment to ensure that the soil is always saturated.

168



169

170

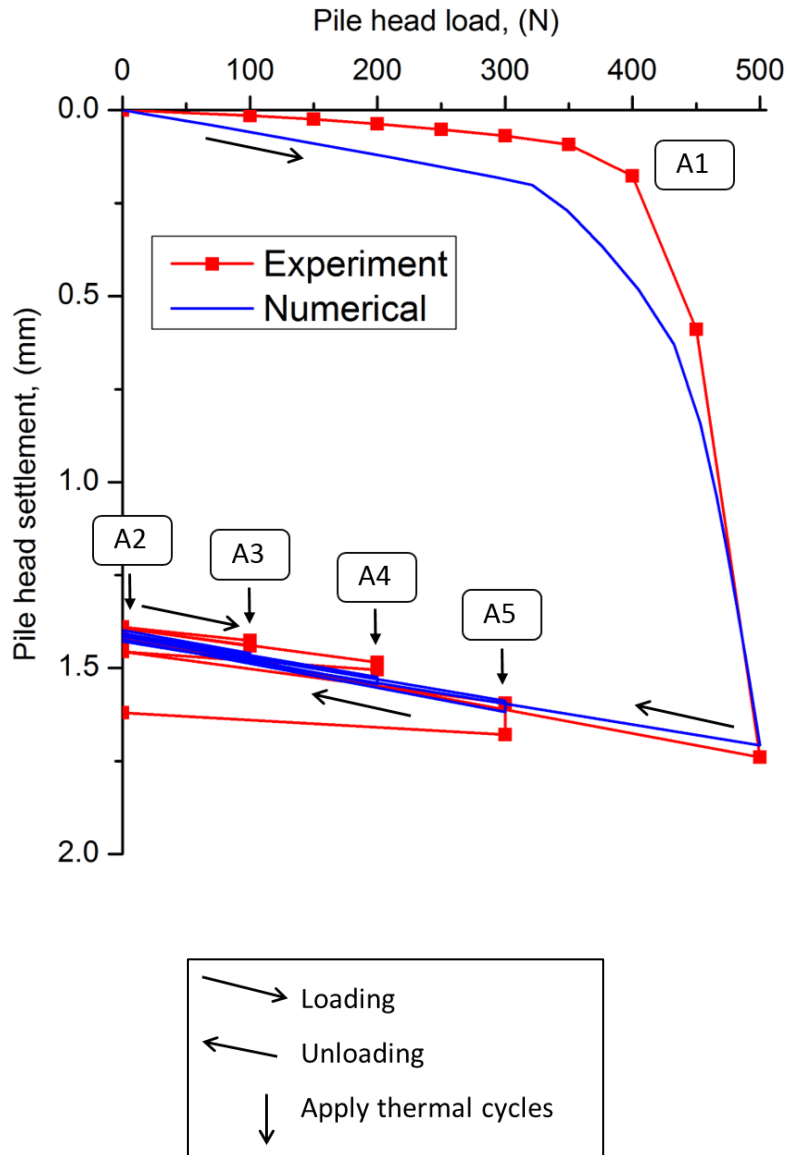
171 **Figure 3.** Evolution of soil suction during the saturation process (measured by tensiometer)

172

173 Before conducting the experiment, temperature of soil and pile was kept at 20 °C for one
174 week. This temperature is close to the room temperature during that period. After the
175 saturation process, the pile was initially subjected to a mechanical load (test A1) to determine
176 its ultimate bearing capacity. A series of load steps was applied to the pile head with
177 increments of 50 N, each loading step being maintained for one hour, following the French
178 Standard (Afnor, 1999). The results, shown in Figure 4, are similar to those obtained by
179 Yavari *et al.* (2016a). That confirms the repeatability of the applied experimental procedure.

180
181
182
183
184
185
186
187
188
189
190
191
192
193

In the test A1, the pile was loaded up to 500 N, which corresponds also to the pile's bearing capacity. After this test, the pile head load was removed. In the test A2, 30 thermal cycles were performed while no load was applied to the pile head. Afterward, the pile head was loaded up to 20% of the pile's capacity prior to the application of 30 thermal cycles (test A3 shown in Figure 4). At the end of these cycles, the pile head load was removed and then a load corresponding to 40% of the pile's capacity was applied. 30 thermal cycles were then performed under this load (test A4). A similar procedure was applied for test A5 corresponding to 60% of pile's capacity. This procedure is similar to that applied by Yavari *et al.* (2016a) where only one thermal cycle was applied per load step. All the five tests were performed on the same soil mass. The mechanical test (A1) was performed at first to identify the pile's capacity. That allowed better define the programme for the subsequent thermo-mechanical tests (A2-A5). Yavari *et al.* (2016a) found that loading the pile to its ultimate bearing capacity and then unload it did not modify its behaviour during the subsequent tests.



194

195

196 **Figure 4.** Pile head load displacement curve: A1 is a purely mechanical test; A2, A3, A4 and

197 A5 are thermo-mechanical tests

198

199 For each thermal cycle, the pile temperature is increased and then decreased with a variation

200 of $\pm 1^\circ\text{C}$ around the initial value (shown later as the thermal sensor S1 in Figure 8). This range

201 is much smaller than the temperature variation of the energy piles which can reach up to

202 $\pm 20^\circ\text{C}$ (Di Donna and Laloui, 2015; Olgun et al., 2015). Actually, in this small-scale model,

203 the dimension of the pile is 20 times smaller than a full-scale pile of 0.4 m in diameter and 12

204 m length. As a consequence, the strain related to the mechanical load is 20 times smaller than

205 that at the full scale (Laloui *et al.*, 2006; Ng *et al.*, 2014). For this reason, the temperature
206 variation was reduced 20 times in order to have a thermal strain of the pile 20 times smaller
207 than that at the full scale. Each thermal cycle is completed within 24 hours, which started
208 with a heating period of 4 hours, and followed by a cooling period of 4 hours, finally the
209 remaining time corresponded to active heating to return to the initial temperature.

210

211 NUMERICAL MODELING

212 *Axisymmetric finite element model*

213 The finite element analysis was performed by using the commercial FEA software, ABAQUS
214 V6.16. To model the physical experiment, two-dimensional axisymmetric model is
215 established (as shown in Figure 5) and fully coupled 4-node temperature-pore pressure-
216 displacement element (CAX4PT) and 4-node bilinear displacement-temperature element
217 (CAX4T) are used for the regions of soil and pile, respectively. Soil is assumed fully
218 saturated throughout the loading cycles and the top 100 mm capillary zone in physical model
219 is ignored. Pore pressure at top surface of soil is opened to air but no heat flow escapes from
220 top surface. Circular hollow section aluminium pile is modelled by solid pile with the
221 equivalent mass density. Soil is modelled by the modified Cam-clay model and the pile is
222 described by linear-elasticity model. For contact properties, the friction coefficient at the soil-
223 pile interface is assumed to be $\tan \phi$, where ϕ is the soil friction angle. Note that a relatively
224 large thermal conductance is chosen at pile-soil interface to reduce the interfacial thermal
225 contact resistance. Lateral pressure coefficient is assumed based on the Meyerhof correlation,
226 $K_0 = (1 - \sin\phi)OCR^{0.5}$, by taking the pressure at 2/3 depth of pile for averaging pressure
227 along the pile to estimate K_0 , and OCR is approximately 160. The calculation of OCR is
228 based on the ratio of the historical maximum pressure and the current experienced pressure.
229 The former is calculated based on the Cam-Clay model parameters from Lv *et al.* (2017), for

230 NCL, *i.e.*, 560 kPa with the experimentally measured void ratio of 0.79. As a result, $K_0=8$ is
 231 adopted for the numerical simulation and it is within a reasonable range since preparation of
 232 physical model involves pre-compaction process. All parameters in simulation are
 233 summarized in Table 1 and Table 2, and the constitutive parameters of soil can be referred to
 234 *Lv et al.* (2017). Initial temperature for the entire numerical model is assumed 20°C as the
 235 case of the physical model. Bottom and side boundaries are set as the constant temperature of
 236 20°C. Deformation of soil is fully fixed at the bottom and only horizontally fixed at the side,
 237 while the top surface is free to deform. Finite sliding formulation is used at soil-pile interface.
 238 Temperature variation with time in physical experiment is deemed to be an input parameter to
 239 investigate settlement occurring under the cyclic thermal loading condition. To simplify the
 240 model, the entire pile is going to experience temperature variation uniformly instead of the
 241 water circulation process in experiment. Thirty heating and cooling cycles are applied in
 242 every thermal loading stage after the given mechanical load. One complete thermal cycle
 243 includes four different thermal phases: initial, heating, cooling, and reheating, which will
 244 induce settlement fluctuation.

245 **Table 1. Parameters of pile and soil in numerical modelling**

Parameters	Pile (CHS aluminium)	Clay (Speswhite Kaolin Clay)
Constitutive model	Linear-elastic	Modified Cam-clay
Dry density (Mg/m ³)	1.32	1.45
Volumetric weight at saturated state (kN/m ³)	N/A	18.53
Young's modulus E (kPa)	1.3E7	N/A
Poisson's ratio ν^*	0.33	0.25
Slope of critical state line M^*	N/A	0.98
Slope of virgin consolidation line	N/A	0.14

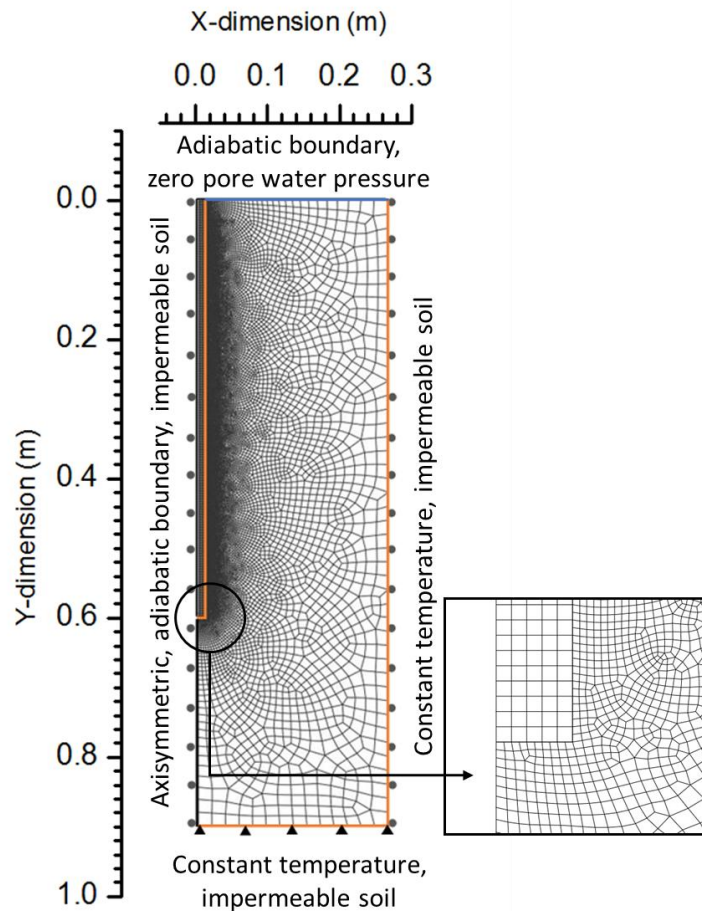
λ^*		
Slope of swelling line κ^*	N/A	0.012
Initial void ratio e_0^*	N/A	1.6
Void ratio after compaction e_1	N/A	0.79
Friction angle ϕ^*	N/A	25°
Permeability k (m/s)*	N/A	1E-8
Thermal expansion (/°C)	2.3E-5	1E-6
Thermal conductivity (W/m°C)	237	1.5
Specific heat capacity (J/kg°C)	9E2	1.269E3

246 * Soil properties are adopted from Lv *et al.* (2017).

247 **Table 2. Other relevant parameters in numerical modelling**

Volumetric weight of water (kN/m ³)	9.81
Friction coefficient $\tan\phi$	0.47
Interfacial thermal conductance (W/°C*m ²)	500
Lateral earth coefficient, K_0	8

248



249

250

Figure 5. Geometry and boundary conditions of the numerical model

251

252 *Mesh sensitivity study*

253

Five different mesh convergence analyses were performed to study mesh dependency of the

254

numerical model. For the pile, uniform 1 mm, 2 mm and 3 mm seed size are applied in the

255

pile region respectively with unchanged 1mm mesh size at soil side of soil-pile interface to

256

find appropriate pile mesh size. It is found that 2 mm mesh size for the pile was sufficient and

257

then, mesh sizes of 1 mm, 1.5 mm and 2 mm are applied into soil side of soil-pile interface

258

region which enables in total 5 different types of mesh size combinations. At the far end,

259

bottom and side of soil, the mesh seed size was set to a fixed 20 mm value for all simulations.

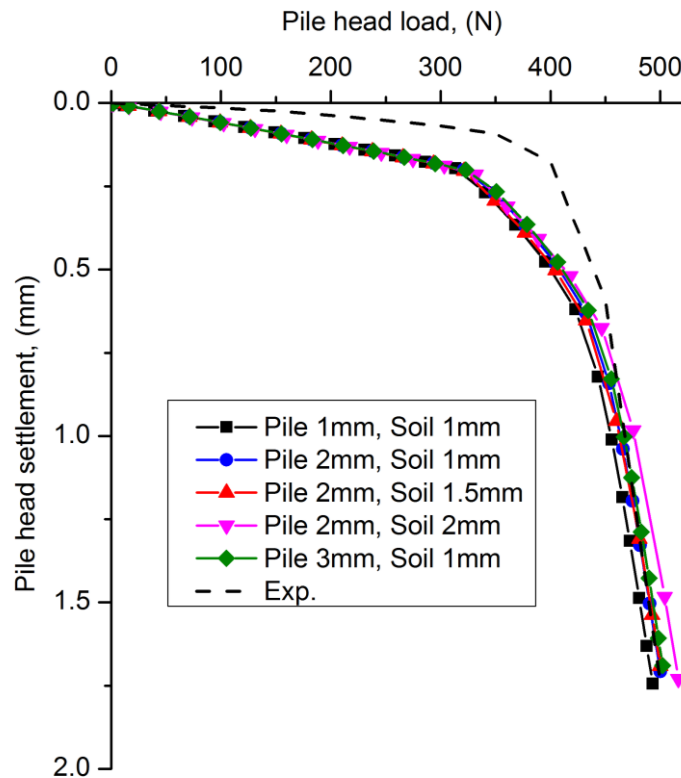
260

Here only the purely mechanical loading condition, A1, was considered for this mesh

261

convergence study, which was similar to Wehnert *et al.* (2004) work. In Figure 6, load and

262 settlement curves for different mesh size combinations are given. The mesh “Pile 2 mm, Soil
 263 1 mm” is selected since it is above the threshold (i.e. Pile 2 mm, soil 1.5 mm) compared with
 264 the experimental data for the pure mechanical loading. This finer mesh provides a better
 265 confidence for the results from later thermo-mechanical analyses, while only slightly
 266 increases the demand on computational resources.



267

268 **Figure 6. Mesh dependency results (A1)**

269 **RESULTS**

270 *Mechanical behaviour of pile*

271 Experiment result (Exp.) of test A1 is shown in Figure 4. This load-settlement curve is based
 272 on the settlement value at the end of each load step. After loading to 500 N the pile is
 273 unloaded and the irreversible settlement of pile head is about 1.42 mm. The relationship
 274 between the axial load and the pile head settlement during the loading is almost linear when

275 the axial load is smaller than 350 N. For axial load higher than this value, pile head
276 settlement increases significantly with the increase of axial load.

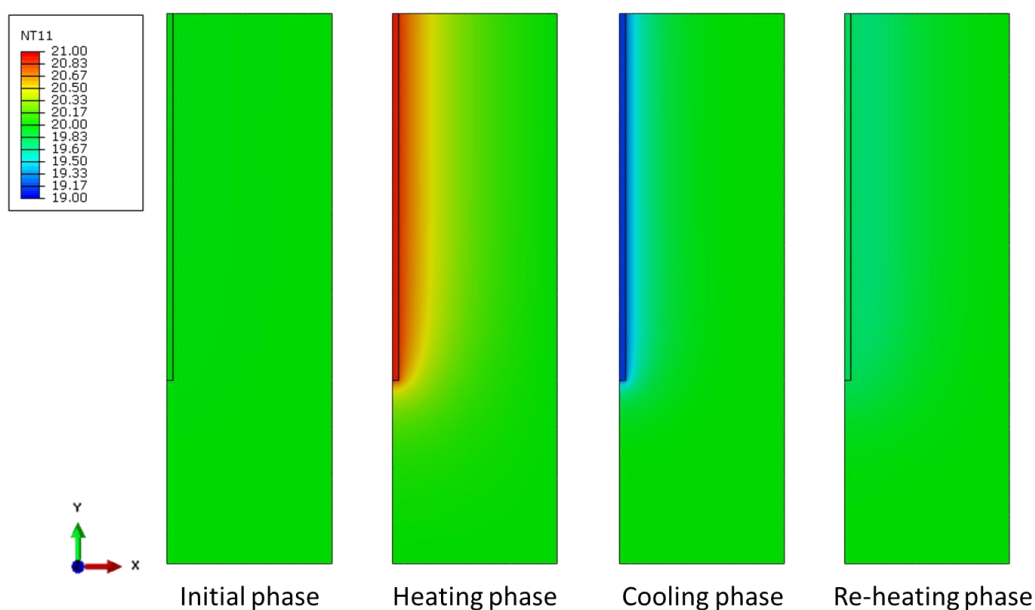
277

278 The numerical result (Num.) gives a similar behaviour of pile by using the parameters of pile
279 and soil shown in Tables 1 and 2. Analysis on the plastic points shows that during the loading
280 path, when the axial load is lower than 350 N, only few plastic points can be observed at the
281 pile toe. Interfacial friction is approaching maximum shear stress. Loading above this value
282 induces development of plastic zones, and this phenomenon can be observed by the quick
283 increase of pile head settlement.

284

285 *Thermo-mechanical behaviour of pile*

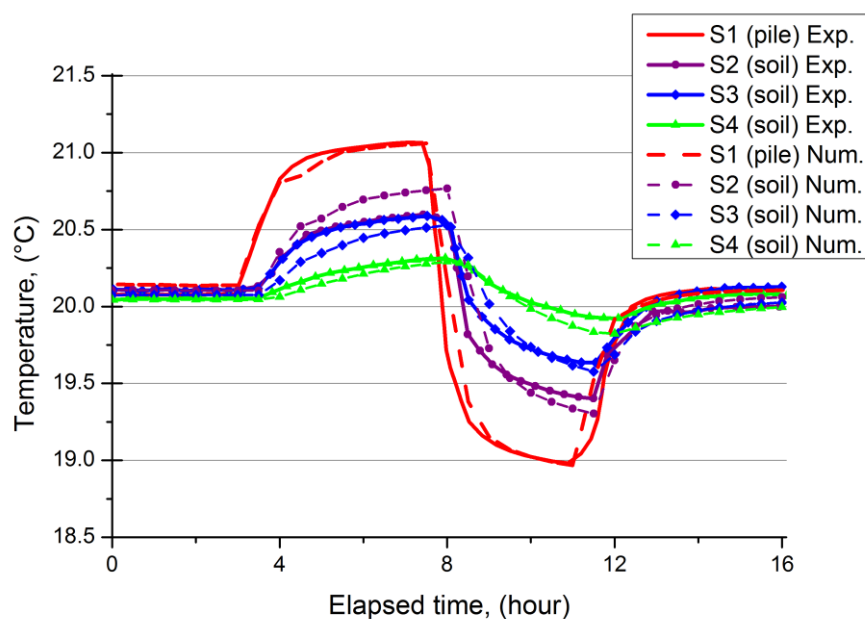
286 In this section, the results of the tests from A2 to A5 are presented. Figure 7 shows the
287 temperature distribution corresponding to four phases of one thermal cycle: initial, heating,
288 cooling, and re-heating. These results confirm that the heat transfer between the pile and the
289 surrounding soil is mainly radial along the pile. Temperature measured at 300-mm depth (in
290 the middle of the pile) should be then representative to study the heat transfer in this study.



291

292 **Figure 7.** Temperature distribution during one thermal cycle obtained from numerical
293 modelling

294 Actually, the Figure 8 presents the temperatures measured at different locations at 300-m
295 depth during one thermal cycle. These measurements evidence that the soil temperature
296 increases when the pile is heated and decreases when the pile is cooled. The effect of pile
297 heating/cooling is more significant for sensors located closer to the pile. The numerical
298 results obtained in the soil are in good agreement with the experimental ones. This agreement
299 confirms that the thermal parameters and the heat transfer mechanisms (heat conduction)
300 used in the numerical model are appropriate. Note that the thermal parameters have been
301 determined separately in laboratory by a thermal probe.



302
303 **Figure 8.** Temperature of pile and surrounding soil during one thermal cycle

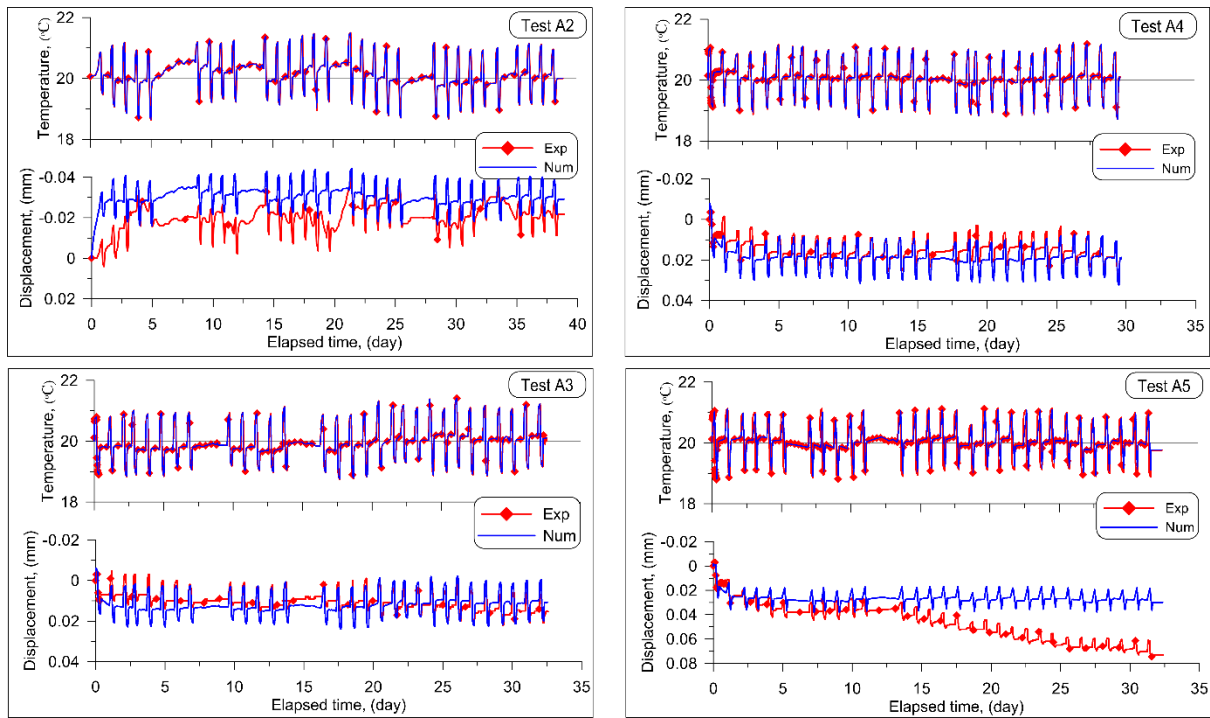
304
305 Figure 9 shows the results of temperature and displacement of the pile over the 30 thermal
306 cycles under different loads. It can be seen that the target temperature (20°C – 21 °C – 19 °C
307 – 20 °C) in each thermal cycle could not be strictly respected during the first test (A2). This is
308 related to the variation of temperature in the room. For this reason, in the subsequent tests

309 (A3, A4, A5) the thermal isolation of the tube connecting the cryostat and the pile was
310 improved, that allowed reducing significantly the influence of room temperature on the pile
311 temperature. In Figure 9, the pile head settlement of each test is set to zero at the beginning of
312 the thermal cycles. The results show generally a pile head heave during heating and
313 settlement during cooling. However, the relation between the pile head displacement and the
314 pile temperature is not strictly reversible. Note that the temperature was controlled manually
315 and for some cycles corresponding to weekend periods the active heating phase took longer
316 than two days. Nevertheless, it seems that these longer phases do not influence significantly
317 the results.

318

319 In the numerical model, the pile temperature measured in the experiment is imposed to the
320 whole pile to simulate the thermal cycles under constant pile head load. The pile head
321 settlement obtained by the simulation is also shown in Figure 9. The numerical results show
322 equally a pile head heave during heating and settlement during cooling. More details on pile
323 head displacement during each thermal cycle and the irreversible pile head displacement are
324 shown in Figure 10 and 11.

325



326

327

Figure 9. Temperature and pile head displacement versus elapsed time (A2-A5)

328

329

To better analyse the pile head displacement during each thermal cycle, in the Figure 10, it is

330

plotted versus pile temperature for the first and the last cycles only. The free expansion curve,

331

obtained with the assumption of a pile restrained at its toe, is also plotted. In each thermal

332

cycle, heating induces pile head heave and cooling induces pile head settlement. For the tests

333

A3, A4, and A5 (under constant head load), the first thermal cycle induces a significant

334

irreversible settlement. For the case of test A2 where not head load was applied, the

335

behaviour during the first thermal cycle is quite reversible. For the last thermal cycle, a

336

reversible behaviour can be observed for all the tests. Besides, it can be noted that the slope

337

of the pile head displacement versus temperature change during the cooling phase is slightly

338

smaller than that of the free expansion curve.

339

The results obtained by the numerical simulation are generally in agreement with the

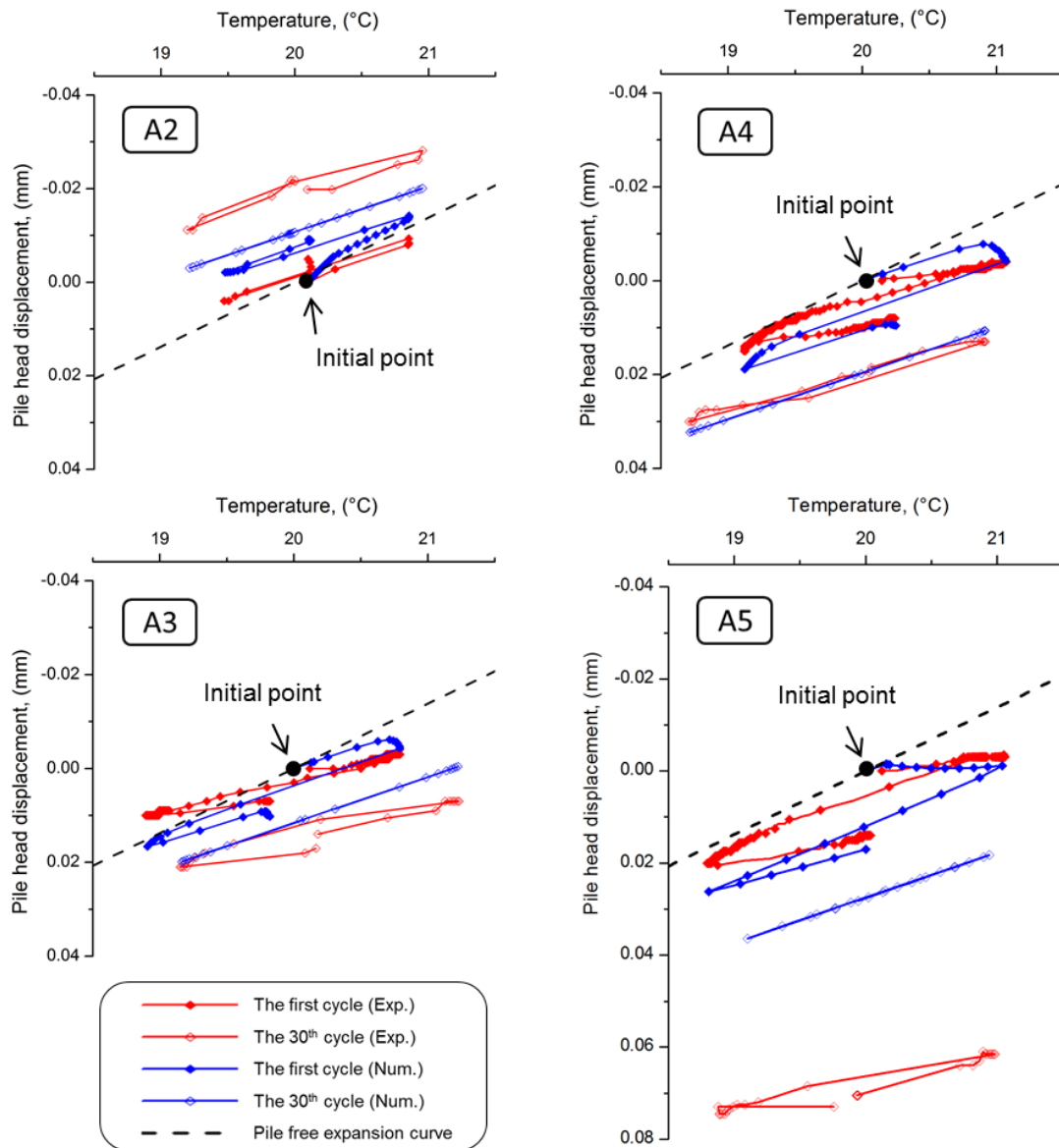
340

experimental ones. Actually, the behaviour obtained during the last thermal cycles is strictly

341

reversible and the first thermal cycle in the tests A3, A4 and A5 (under constant pile head

342 load) induces significant reversible settlement. Only the behaviour of the first cycle of test A2
 343 (without pile head load) show a difference. In the numerical model, an irreversible pile head
 344 heave was obtained after the first thermal cycle.
 345

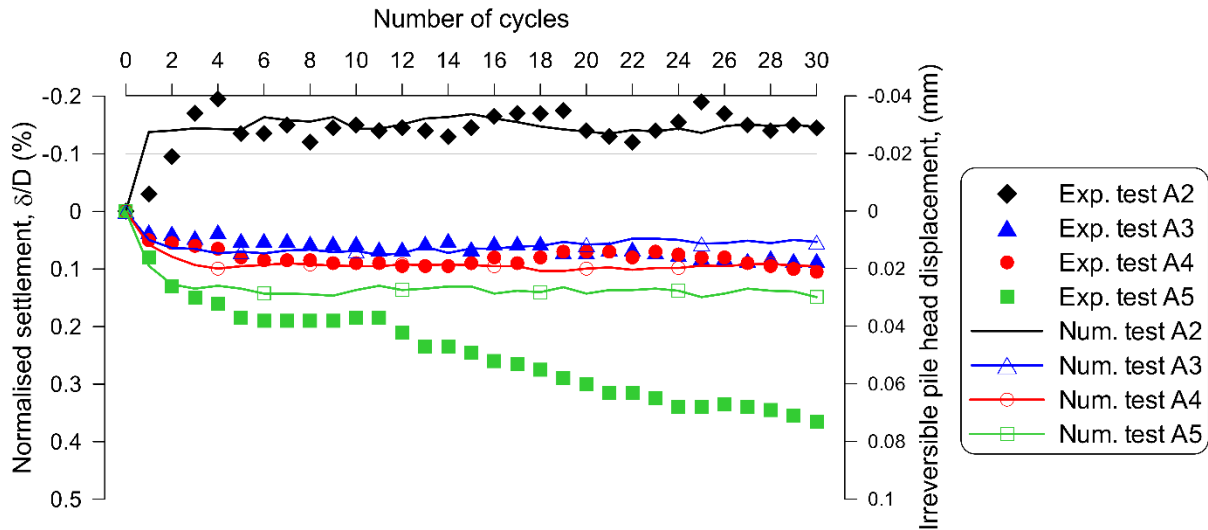


346
 347 **Figure 10.** Pile head settlement versus pile temperature during the first and the 30th cycles
 348
 349 The irreversible pile head displacement is plotted versus the number of cycles in the Figure
 350 11. For a better comparison with full-scale experiments, it is also normalised with the pile

351 diameter. For the test A2, the first cycle induces pile head heave up to 0.15% of pile diameter
352 with the numerical model. Afterward, the pile behaviour remains reversible during thermal
353 cycles. However, with the physical model, the first cycle induces only very small pile heave
354 (0.03% of pile diameter). But pile heave continues to increase during the subsequent cycles
355 and reaches 0.20% of pile diameter after four cycles. For the tests A3 and A4, the first
356 thermal cycles induce significant irreversible settlement. This latter become negligible for the
357 subsequent cycles. The behaviour of the pile in the test A5 is also similar to that of tests A3
358 and A4. However, after the tenth cycle, the irreversible settlement increases continuously
359 with the increase of the number of cycles. Besides, it can be noted that the irreversible
360 settlement depends on the pile head load; the higher the pile head load the higher the
361 irreversible settlement. For the test A5, the sudden increase of irreversible settlement from
362 the 10th cycle should be related to some technical problems. The possible causes of problems
363 occurred could be: tilting of the pile at high cumulative settlement, failure of soil around the
364 pile toe, or other physico-chemical phenomena that occur in soil after a long period (several
365 months).

366

367 The results obtained by the numerical simulation are generally in good agreement with the
368 experimental ones. The only difference is related to the test A5 where the pile head
369 irreversible displacement remains constant event after the tenth cycle in the numerical
370 simulation.



371

372

Figure 11. Irreversible pile head displacement versus number of thermal cycles

373

374 The long-term performance of the pile is further illustrated according to the numerical results.

375 Vertical displacement of pile length on heating phase (H), cooling phase (C) and reheating

376 phase (R) are plotted in Figure 12. The first, second, twentieth and thirtieth thermal cycles are

377 selected here because simulation results show that the majority of irreversible settlement

378 happens within the first-three cycles and is relatively stable in the rest of thermal cycles. Note

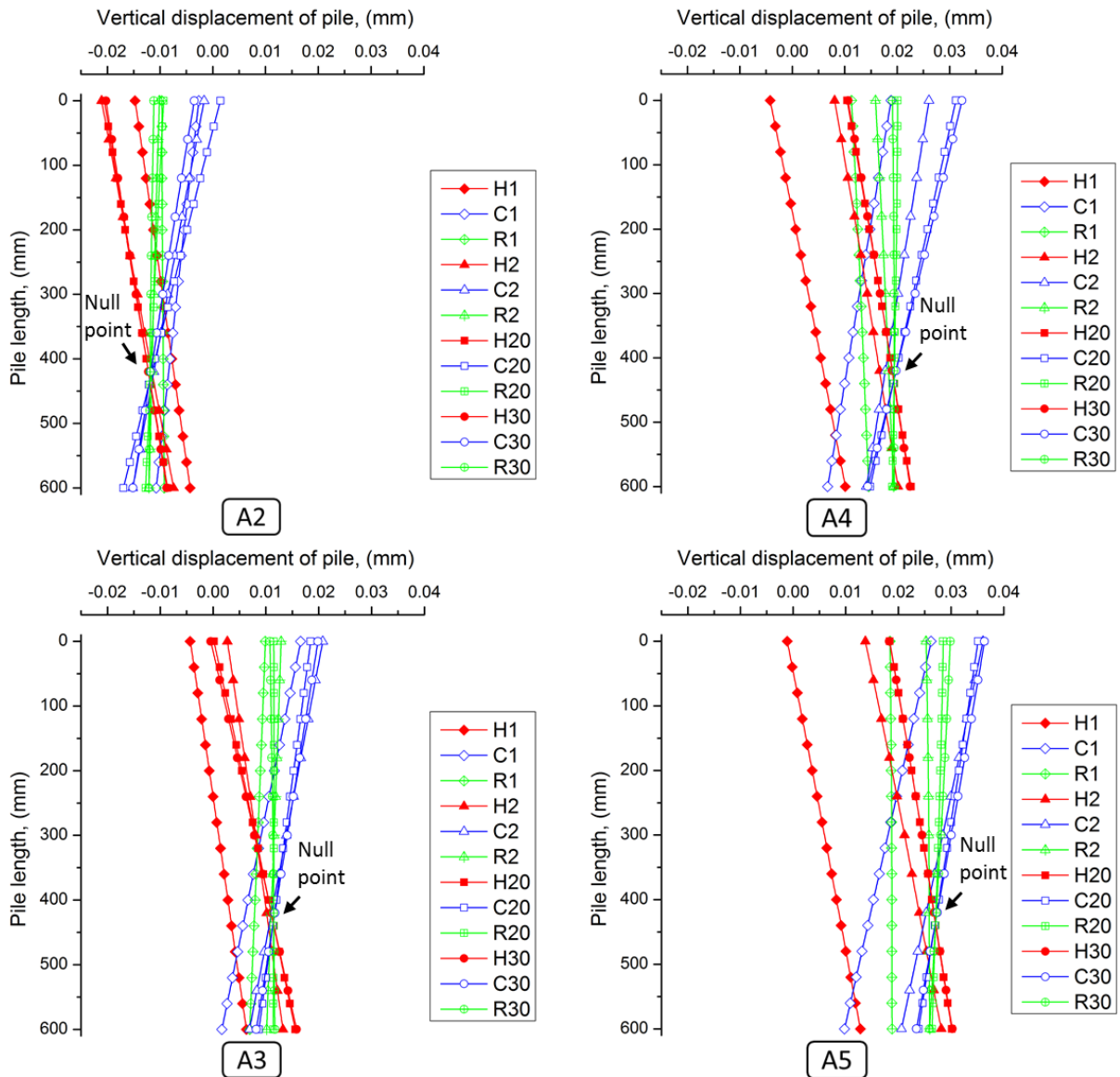
379 that the vertical displacement of pile is assumed zero at the beginning of first cycle in order to

380 be consistent with Figure 11. It is obvious that heating and cooling the pile cause

381 displacement distribution to be mirror-reflecting each other and vertical displacement remains

382 constant along pile length in reheating phase. The time evolution of displacement profile is

383 stabilised over a few cycles with a null point at about 430 mm beneath the top surface.



384

385

Figure 12. Vertical displacement along the pile length (numerical results)

386

387 The total vertical stress along the pile length under different thermal cycles obtained from the

388 numerical simulation is presented in Figure 13. Only the results obtained from the first and

389 the last cycles are presented for clarity. Generally, heating the pile induces a slight increase of

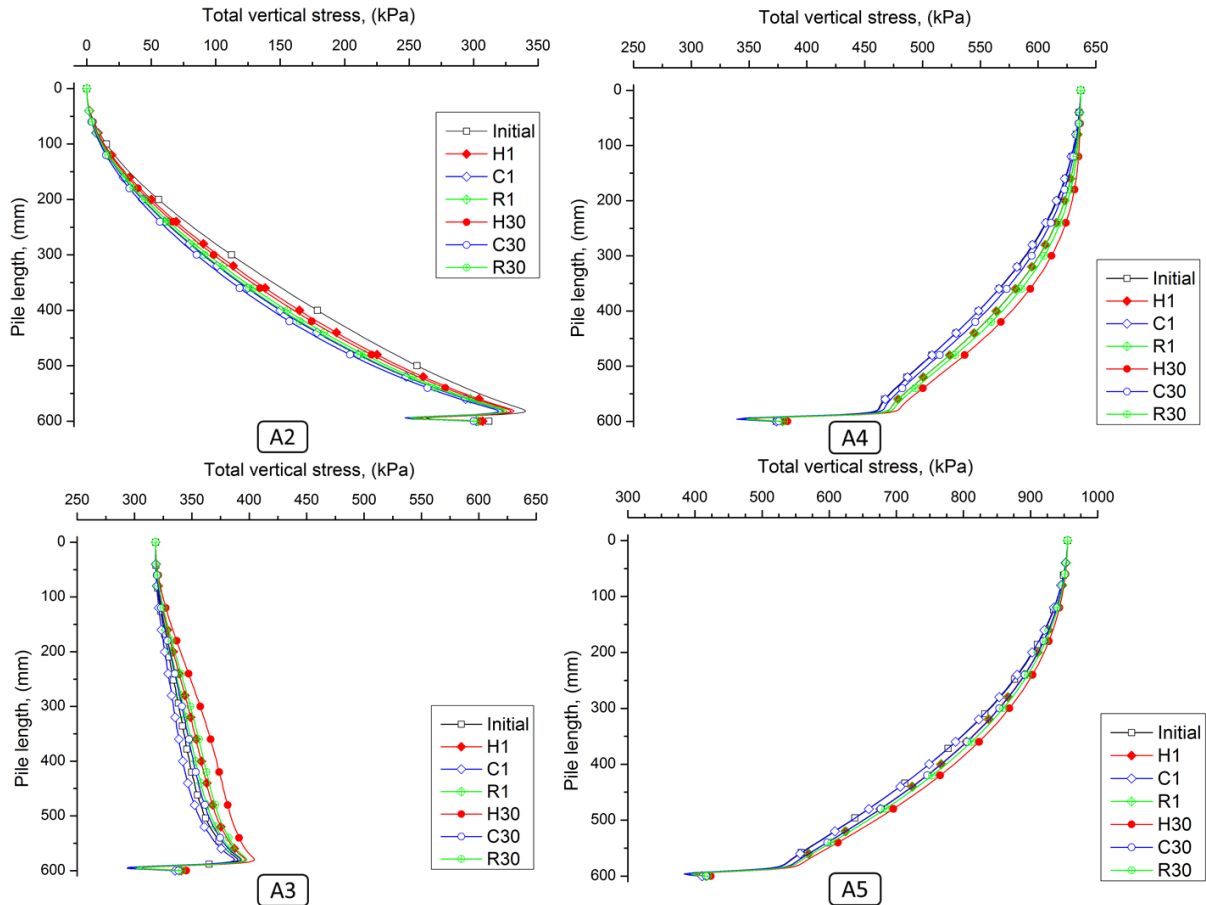
390 vertical stress and cooling causes a decrease in vertical stress distribution along the pile

391 length. The behaviour obtained during the first cycle of test A2 is slightly different; heating

392 induces a decrease of vertical stress and cooling decreases again this latter. Besides, the

393 vertical stress is observed to slightly increase from the first to the last thermal cycles in all
394 heating, cooling and reheating phases.

395



396

397 **Figure 13.** Thermal effect on the total vertical stress along the pile length (numerical results)

398

399 DISCUSSION

400

401 In the mechanical test paths (test A1), the material parameters for the numerical simulation
402 are adopted from Lv *et al.* (2017). From the results, it is obvious that the estimated bearing
403 capacity is in agreement with the experimental results (Figure 4). A carefully estimated
404 lateral stress coefficient (K_0) is important to consider the compaction process in physical
405 model.

406

407 In the test A2, the upward displacement of pile (as shown in Figure 9) during heating/cooling
408 cycles, observed on both physical and numerical models, can be explained by the stress state
409 shown in Figure 13. Actually, the test A2 starts after the mechanical unloading path of test
410 A1. At the end of the unloading path, the pile is still subjected to compressive stress (up to
411 300 kPa at its toe). Thermal cycles in test A2 induce thermal dilation/contraction of the pile.
412 This movement would release this compressive stress and heave the pile. The results shown
413 in Figure 13 evidence this stress release after thermal cycles.

414

415 In the subsequent tests (A3, A4, A5), irreversible settlement was observed during the first
416 thermal cycles. These results are in agreement with those observed by Ng *et al.* (2014) (using
417 centrifuge modelling) and Vieira & Maranha (2016) by using the finite element method.
418 However, only five thermal cycles were investigated in these works. Actually, the axial stress
419 profiles plotted in Figure 13 show that these thermal cycles increase the axial stress along the
420 pile. That means the thermal dilation/contraction of the pile facilitate the transmission of axial
421 pile head load to the pile toe. In the present works, both numerical and physical models show
422 that the pile settlement becomes reversible under thermal cycles at high number of cycles
423 (except for the test A5).

424

425 The numerical model shows behaviour similar to that obtained by physical model; the pile
426 settlement progressively achieves stable state due to densification process in each thermal
427 cycle. Especially the first thermal cycle shows good agreement with the experimental result
428 (Figure 10). The explanation of why numerical simulation is able to predict progressive
429 settlement owes to the use of the modified Cam-clay model as the constitutive model for soil.
430 The Cam-clay criterion follows the poro-plasticity rule that could more effectively simulate

431 densification process during thermal cyclic loads. Whereas Mohr-Coulomb model may not
432 well describe such soil behaviour (Yavari *et al.*, 2014). Therefore, the present numerical
433 prediction of long-term thermal cyclic settlement of energy pile is able to predict
434 experimental data with relatively good agreement.

435

436 The results of Figure 10 show that the slope of the pile head displacement versus temperature
437 change during the cooling phase is slightly smaller than that of the free expansion curve.
438 Actually, similar tests on dry sand have shown that this slope is similar to the free expansion
439 curve (Kalantidou *et al.*, 2012; Yavari *et al.*, 2014). The behaviour observed in the present
440 work can be explained by the results shown in Figure 12. Actually, the null-point does not
441 locate at the pile toe but at 400 – 450 mm depth. For this reason, the pile head displacement
442 does not correspond to the free expansion of the whole pile length.

443

444 In the present work, the numerical model was able to reproduce correctly the thermo-
445 mechanical behaviour of a small-scale energy pile under several thermal cycles. Note that the
446 range of the temperature variation in the physical model was limited to ± 1 °C. This value is
447 much smaller than full-scale application (up to ± 20 °C) in order to respect the scale effect.
448 Within this limited range of temperature variation, the soil parameters can be assumed to be
449 independent of temperature. However, for a higher temperature variation, the temperature
450 change can slightly modify the soil properties (Tang *et al.*, 2008; Vega & McCartney, 2015;
451 Hong *et al.*, 2016; Yavari *et al.*, 2016b; Jacinto & Ledesma, 2017; Ghorbani *et al.*, 2019).
452 The use of the present numerical model to predict the behaviour of real-scale energy
453 foundations should consider this aspect.

454

455 Results obtained in the present study would be helpful for studies on various types of thermo-
456 active geostructures (Hoyos *et al.*, 2015; Narsilio *et al.*, 2017; Sanchez *et al.*, 2017; Angelotti
457 and Sterpi, 2019; Baralis *et al.*, 2019)

458

459 CONCLUSIONS

460 The long-term thermo-mechanical behaviour of energy pile is investigated in the present
461 work by using a small-scale model pile (physical modelling) and the finite element method
462 (numerical modelling). The following conclusions can be drawn:

- 463 ✓ Thermal cycles applied to the pile under constant pile head load induce stress
464 redistribution inside the pile. That can induce irreversible pile heave in the case
465 without pile head load and irreversible pile settlement in the case with pile head load.
- 466 ✓ The irreversible pile head settlement/heave is more important within the first thermal
467 cycles; it becomes negligible at high number of cycles.
- 468 ✓ The main mechanism that controls the soil/interaction during thermal cycles under
469 constant pile head load is the pile thermal contraction/dilation. The numerical model
470 can capture correctly the experimental result without considering the temperature
471 effect on soil's parameters.

472 The preliminary results shown in this paper could warrant future numerical studies for the
473 serviceability design of geothermal energy piles.

474

475 ACKNOWLEDGEMENT

476 Dr. Gan acknowledges the financial support of Labex MMCD for his stay at Laboratoire
477 Navier. Labex MMCD benefits from a French government grant managed by ANR within the
478 frame of the national program Investments for the Future ANR-11-LABX-022-01.

479

480 REFERENCES

- 481 Abuel-Naga H, Raouf MIN, Raouf AMI, Nasser AG (2015) Energy piles: current state of
482 knowledge and design challenges, *Environmental Geotechnics*, 2(4), 195- 210.
- 483 AFNOR (1999) Essai statique de pieu isolé sous un effort axial, NF P 94-150-1, 28 pages.
- 484 Angelotti A and Sterpi D (2019). On the performance of energy walls by monitoring
485 assessment and numerical modelling: a case in Italy. *Environmental Geotechnics*, doi:
486 10.1680/jenge.18.00037.
- 487 Baralis M, Barla M, Bogusz W, Di Donna A, Ryzynski G & Zerun M (2019). Geothermal
488 potential of the NE extension Warsaw (Poland) metro tunnels. *Environmental*
489 *Geotechnics*, doi: 10.1680/jenge.18.00042.
- 490 Bidarmaghz A, Francisca FM, Makasis N and Narsilio GA (2016) Geothermal energy in
491 loess, *Environmental Geotechnics*, **3(4)**, 225 – 236, doi:10.1680/jenge.15.00025.
- 492 De Santayana FP, de Santiago C, de Groot M, Uchueguia J, Acros JL and Badenes B (2019).
493 Effect of thermal loads on pre-cast concrete thermopile in Valencia, Spain,
494 *Environmental Geotechnics*, doi: 10.1680/jenge.17.00103.
- 495 Di Donna A, and Laloui L (2015) Numerical analysis of the geotechnical behaviour of energy
496 piles, *Int. J. Numer. Anal. Methods Geomech.*, **39(8)**, 861–888, doi:10.1002/nag.2341.
- 497 Ghorbani J, El-Zein A and Airey DW (2019) Thermo-elasto-plastic analysis of geosynthetic
498 clay liners exposed to thermal dehydration. *Environmental Geotechnics*, doi:
499 10.1680/jenge.17.00035.
- 500 Hoyos LR, DeJong JT, McCartney JS, Puppala AJ, Reddy KR & Zekkos D (2015)
501 Environmental geotechnics in the US region: a brief overview. *Environmental*
502 *Geotechnics*, **2(6)**, 319 – 325, doi: 10.1680/envgeo.14.00024.
- 503 Hong PY, Pereira JM, Cui YJ and Tang AM (2015) A two-surface thermomechanical model
504 for saturated clays. *International Journal for Numerical and Analytical Methods in*
505 *Geomechanics*, **40(7)**, 1059-1080, doi: 10.1002/nag.2474.
- 506 Jacinto AC and Ledesma A (2017). Thermo-hydro-mechanical analysis of a full-scale heating
507 test. *Environmental Geotechnics*, 4(2), 123 – 134, doi: 10.1680/jenge.15.00049.
- 508 Kalantidou A, Tang AM and Pereira JM (2012) Preliminary study on the mechanical
509 behaviour of heat exchanger pile in physical model. *Géotechnique*, **62(1)**, 1047-1051,
510 doi.org/10.1680/geot.11.T.013.
- 511 Laloui L, Nuth M and Vulliet L (2006) Experimental and numerical investigations of the
512 behaviour of a heat exchanger pile. *International Journal for Numerical and Analytical*
513 *Methods in Geomechanics*, **30(8)** 763-781, doi: 10.1002/nag.499

- 514 Lv YR, Ng CWW, Lam SY, Liu HL and Ma LJ (2017) Geometric Effects on Piles in
515 Consolidating Ground: Centrifuge and Numerical Modeling. *Journal of Geotechnical*
516 *and Geoenvironmental Engineering*, **143(9)**, 04017040.
- 517 Narsilio GA, Sanchez M, Alvarellos J and Guimaraes L (2017) Editorial: XV Pan-American
518 Conference: selected papers on energy geotechnics. *Environmental Geotechnics*, **4(2)**,
519 67 – 69, doi: 10.1680/jenge.2017.4.2.67.
- 520 Ng, CWW, Shi C, Gunawan A, and Laloui L (2014) Centrifuge modelling of energy piles
521 subjected to heating and cooling cycles in clay, *Géotechnique Letters*, **4(4)** 310–316,
522 doi:10.1680/geolett.14.00063.
- 523 Ng CWW, Ma QJ and Gunawan A (2016) Horizontal stress change of energy piles subjected
524 to thermal cycles in sand. *Computers and Geotechnics*, **78 (2016)**, 54–61,
525 doi:10.1016/j.compgeo.2016.05.003.
- 526 Nguyen VT, Tang AM and Pereira JM (2017) Long-term thermo-mechanical behavior of
527 energy pile in dry sand. *Acta Geotechnica*, **12(4)**, 729 – 737.
- 528 Olgun CG, Ozudogru TY, Abdelaziz SL and Senol A (2015) Long-term performance of heat
529 exchanger piles, *Acta Geotechnica*, **10(5)**, 553–569, doi:10.1007/s11440-014-0334-z.
- 530 Pasten C, Shin H, and Santamarina JC (2013) Long-Term Foundation Response to Repetitive
531 Loading, *J. Geotech. Geoenvironmental Eng.*, **140(4)**, 4013036,
532 doi:10.1061/(ASCE)GT.1943-5606.0001052.
- 533 Pasten C, and Santamarina JC (2014) Thermally Induced Long-Term Displacement of
534 Thermoactive Piles, *J. Geotech. Geoenvironmental Eng.*, **140(5)**, 6014003,
535 doi:10.1061/(ASCE)GT.1943-5606.0001092.
- 536 Saggi R, and Chakraborty T (2015) Cyclic Thermo-Mechanical Analysis of Energy Piles in
537 Sand. *Geotechnical and Geogical Engineering*, **33(2)**, 321–342, doi:10.1007/s10706-
538 014-9798-8.
- 539 Sanchez M, Falcao F, Mack M, Pereira JM, Narsilio GA and Guimaraes L (2017) Salient
540 comments from an expert panel on energy geotechnics. *Environmental Geotechnics*,
541 **4(2)**, 135 – 142, doi: 10.1680/jenge.16.00008.
- 542 Suryatriyastuti ME, Mroueh H, and Burlon S (2014) A load transfer approach for studying
543 the cyclic behavior of thermo-active piles. *Computers and Geotechnics*, **55**, 378–391,
544 doi:10.1016/j.compgeo.2013.09.021.
- 545 Tang AM, Cui YJ and Barnel N (2008) Thermo-mechanical behaviour of compacted swelling
546 clay. *Géotechnique*, **58(1)** 45-54, doi: [10.1680/geot.2008.58.1.45](https://doi.org/10.1680/geot.2008.58.1.45)
- 547 Vega A and McCartney JS (2015) Cyclic heating effects on thermal volume change of silt.
548 *Environmental Geotechnics*, **2(5)**, 257 – 268, 10.1680/envgeo.13.00022.

- 549 Vieira A and Maranhã JR (2016) Thermoplastic Analysis of a Thermoactive Pile in a
550 Normally Consolidated Clay. *International Journal of Geomechanics.*, **17(1)** 4016030,
551 doi:10.1061/(ASCE)GM.1943-5622.0000666.
- 552 Yavari N, Tang AM, Pereira JM and Hassen G (2014) Experimental study on the mechanical
553 behaviour of a heat exchanger pile using physical modelling, *Acta Geotechnica*, **9(3)**,
554 385–398, doi:10.1007/s11440-014-0310-7.
- 555 Yavari N, Tang AM, Pereira JM and Hassen G (2016a), Mechanical behaviour of a small-
556 scale energy pile in saturated clay, *Géotechnique*, **66(11)**, 878-887,
557 doi:10.1680/jgeot.15.T.026.
- 558 Yavari N, Tang AM, Pereira JM and Hassen G (2016b) Effect of temperature on the shear
559 strength of soils and soil/structure interface. *Canadian Geotechnical Journal*, **53(7)**,
560 1186-1194, doi:10.1139/cgj-2015-0355.
- 561 Wehnert M and Vermeer PA (2004) Numerical analyses of load tests on bored piles.
562 *Numerical methods in geomechanics*–NUMOG IX, 505-511.
- 563
- 564